Specific absorption rate and Path Loss in specific body location in Heterogeneous Human Model

Divya Kurup, Wout Joseph, Günter Vermeeren, and Luc Martens

IBBT-Ghent University, Dept. of Information Technology

Gaston Crommenlaan 8 box 201, B-9050 Ghent, Belgium

Fax: +32 9 33 14899, E-mail: divya.kurup@intec.UGent.be

Abstract

A multi implant scenario is considered using insulated dipole antennas for specific locations such as the liver, heart, spleen, and the kidneys where implants communicate with a pacemaker acting as a central hub. Wireless communication within human body experiences loss in the form of attenuation and absorption, and to identify these losses, the path loss (PL) is studied in this paper for an adult and child heterogeneous human model. Link performance is calculated to investigate the applicability of in-body communication. The specific absorption rate for all these locations is also studied in order to verify compliance with international safety guidelines.

I. Introduction

A wireless body area network (WBAN) is a network, consisting of nodes that communicate wirelessly and are located on or in the body of a person. There are various applications for such a network in areas of medicine, sports, and multimedia [1].

Active implants are positioned at specific locations inside the human body to carry out special tasks such as drug delivery, transplanted organ monitoring, and functional electrical stimulation. In case of liver

transplantation, implants are placed on the liver for constant monitoring for a period of 7-10 days to report circulation deficiency to physicians [2]. This can also be the case for other organs that undergo transplantation where constant monitoring is required before and after the surgical procedure. An implant such as a glucose sensor which transmits blood glucose data wirelessly helps diabetic patients to control their blood sugar level. Such implants can exist by themselves at a specific location or co-exist with other implants in the human body (e.g, pacemaker with organ monitoring sensor or glucose sensor). Considering a multi-implant case, the implants can communicate with the pacemaker/central hub present in the body which then can communicate with a receiver placed outside the body. Implants such as pacemakers and implantable cardioverter defibrillators (ICDs) also need to relay information for control or monitoring to devices placed outside the body. The transfer of data from the in-body implants to the receiver placed outside the body thus only need to take place from one of the in-body implant, for example a pacemaker that collects all data. This reduces the need for various sensors to communicate with receiver outside the body. For an efficient communication between the sensors, an accurate characterization of the propagation channel is necessary. Some good research have been performed in WBAN research areas [3]–[5], however till date, characterization of the propagation channel for multiple in-body sensors has not been performed. Thus a proper and efficient modeling of the channel is required for the performance analysis of in-body sensor networks. A path loss (PL) model helps to gauge the reliability of the link between nodes placed within or on the human body.

In addition to PL, we study absorption as various health risks are related to exposure from strong radiofrequency (RF) electromagnetic (EM) fields. This absorption, characterized by the SAR (Specific Absorption Rate) [W/kg], is limited by standards such as those of the Institute of Electrical and Electronics Engineers (IEEE) [6] and the guidelines provided by the International Commission on Non-Ionizing Radiation Protection (ICNIRP) [7] to avoid excessive heating in the human body.

There is an extensive literature on modeling of propagation loss within the human body [8]–[11]. Various scenarios are considered in these works however none of them provide any PL models for a multi-implant

scenario which takes specific organs into consideration. [9] suggests a PL model for in-body wireless implants. However it does not make use of biocompatible implantable antennas. A PL model for in-body wireless implants by making use of insulated dipole antennas in a homogeneous medium is proposed in [10]. [11] provides various scenarios for channel modeling for an endoscopy application, however does not make use of an insulated antenna and develops a PL model with a high standard deviation of 7.3 dB.

The goal of this paper is to develop an empirical PL model for a heterogeneous human model at 2.45 GHz, using insulated dipole antennas with respect to specific locations of selected organs and to also suggest the maximum deviation that can be obtained for placement of an implant. We select the 2.45 GHz frequency corresponding to the Industrial, Scientific, and Medical (ISM) band as this is one way to reduce the antenna size and make it available to be implanted. Another advantage is that the larger bandwidth allows for higher bitrates. Various antennas are manufactured for the same reason [12]–[14] . It is also noticed that in the study of absorption at lower frequencies ($<$ 450 MHz) there was increased SAR in layered tissue which diminishes at higher frequencies [15]. The recent voting by FCC to include 2.36-2.4 GHz spectrum in Medical Device Radiocommunications (MedRadio) for body area networks is also a motivation as this means that a whole new market is going to be opened and thus making such a study valuable.

The novelty of the study is that it takes into consideration location specific PL for the organs of human body. Since it is difficult to carry out measurements in the human body this study is carried out using finite difference time domain (FDTD) simulations. We select various vital organs such as kidney, heart, spleen, and liver as these are the most transplanted organs for the study of path loss between a transmitter (Tx) antenna placed at the periphery of these organs and a receiver (Rx) antenna that is placed at a location of a pacemaker (left shoulder area below the pectoral muscle). For every location of the Tx antenna, the peak spatial-averaged SAR has been assessed in order to check compliance with international safety guidelines.

II. Heterogeneous Medium: Setup and configuration

We developed two identical insulated dipole antennas [10], [16], where the dipole arms are perfect electric conductors (PEC) surrounded with an insulation made of polytetrafluoroethylene (relative permittivity $\epsilon_r = 2.07$ and conductivity $\sigma = 0$ S/m). We use dipole antennas for our study as they are the best understood antennas in free space and have a simple structure. Since it is difficult to carry out measurements using heterogeneous human models the antennas are developed for homogeneous muscle tissue medium ($\epsilon_r = 50.8$ and $\sigma = 2.01$ S/m [17]). Resonance is obtained for the insulated dipole antennas with length ℓ_1 = 3.9 cm, at a frequency of 2.457 GHz. Insulated dipoles are selected instead of bare dipoles because the insulation prevents the leakage of conducting charges from the dipole and reduces the sensitivity of the entire distribution of current to the electrical properties of the ambient medium. This property makes insulated dipoles valuable for WBAN purposes [10], [18].

The location plays a vital role as the implants cannot be randomly placed within the human body. Taking into consideration the various in-body sensors used and the transplanted organs, the best position of the implants selected to carry out this study is at the periphery of the vital organs. The placement of the implant should be such that no harm is caused to the vital organs and the body functions. The Rx will be placed at a fixed location of a pacemaker/central hub such that a link is established between the vital organs and the pacemaker/central hub. And the Tx is placed at various positions around the periphery of the vital organs considered.

Simulations are carried out using a 3D electromagnetic solver SEMCAD-X (SPEAG, Switzerland), a finite-difference time-domain (FDTD) program.

The PL in heterogeneous medium is investigated using an enhanced anatomical model of a 34 year adult, Virtual family man (VFM), and a 6 year male child Virtual family boy (VFB) from the $Virtual\ Family$ [19] at 2.45 GHz. The VFM has a height of 1.74 m and a weight of 70 kg. The model consists of more than 80 different tissues. Fig. 1 shows the organs on whose periphery the Tx antenna is placed and also the position of the Rx. The VFB has a height of 1.17 m and a weight of 19.5 kg. The model consists

of 81 different tissues. The positions of the Tx on the different organs are as follows:

- $Liver$: The Tx is placed on the periphery of the liver as shown in the Fig. 1. The liver is the largest internal and the heaviest organ in the human body. The positions are selected in the following manner. The vertical positions on the liver as shown in Fig. 1 are separated by a distance of 10 mm each and the horizontal positions are separated by 10 mm each. In this manner the whole organ is covered. This method is used for all other organs. The Tx antenna is placed in parallel with respect to the Rx at 100 different positions on the periphery of the liver. In the child the organs are much smaller than that of an adult and thus in order to have more samples we have placed the horizontal positions 5 mm apart. The Tx antenna is placed in parallel with respect to the Rx at 134 different positions on the periphery of the liver.
- $Left\ Kidney$: The left kidney is situated towards the posterior side of the abdominal cavity on the left side, just above the waist and is also shown in Fig. 1. The Tx antenna is placed in parallel to the Rx at 25 different positions on the periphery of the left kidney for the VFM and for 22 positions for the VFB.
- $Right\ Kidney$: The right kidney is situated towards the posterior side of the abdominal cavity on the right side, just above the waist and is shown in Fig. 1. The Tx antenna is placed in parallel to the Rx at 25 different positions on the periphery of the right kidney in the VFM and 30 different positions for the VFB
- $Spleen$: The spleen is located below the diaphragm and above the left kidney and can be seen in Fig. 1. The Tx antenna is placed at 26 different positions in the VFB and 24 different positions in the VFB.
- $Heart$: The heart is located just behind and slightly towards the left of the breastbone. The Tx antenna is placed at 36 different positions with the same 10 mm separations as above in the VFM and for 55 positions for the VFB.

III. Results

A. Path Loss

PL is defined as the ratio of input power at port 1 (P_{in}) to power received at port 2 (P_{rec}) in a two-port setup. PL in terms of transmission coefficient is defined as $1/|S_{21}|^2$ with respect to 50 Ω when the generator at the Tx has an output impedance of 50 Ω and the Rx is terminated with 50 Ω. This allows us to regard the setup as a two-port circuit for which we determine $|S_{21}|_{\mathrm{dB}}$ with reference impedances of 50 Ω at both ports.

$$PL|_{\mathrm{dB}} = (P_{in}/P_{rec}) = -10\ \log_{10}|S_{21}|^2 = -|S_{21}|_{\mathrm{dB}}, \tag{1}$$

PL is represented for the periphery of each vital organ with the help of boxplots. For each box the bottom and top of the box represents the lower and upper quartiles, respectively. The band at the middle of the box represent the median. The whiskers of the box represents the minimum and the maximum value and any data that lies beyond the whiskers are the outliers. The boxplots thus show the variation of the PL for each organ through its five-number description statistics, i.e, the minimum, the lower quartile, the median, the upper quartile and the maximum of the PL samples all in dB.

B. Validation

In order to validate the simulation tool and antenna models used, measurements are performed in homogeneous muscle tissue at a frequency of 2.45 GHz. Measurements are executed using a vector network analyzer NWA (Rohde and Schwarz ZVR) and the scattering parameters $|S_{11}|_{dB}$ and $|S_{21}|_{dB}$ (with respect to 50 Ω) between transmitter (Tx) and the receiver (Rx) for the different separations are determined. The path loss is then calculated from $|S_{21}|_{dB}$. A flat phantom, representing the trunk of a human body and recommended by CENELEC standard EN50383 (dimensions 80×50×20 cm^3), is filled with muscle tissue simulating fluid (relative permittivity = 50.8 and conductivity = 2.01 S/m at 2.45 GHz). The two insulated dipoles are immersed, placed parallel and lined up for maximal power transfer at 5 cm above the bottom of the flat phantom. Simulations are performed using the 3D electromagnetic solver

SEMCAD-X, finite-difference time-domain (FDTD) program and FEKO a method of moment (MoM) program. The deviations between the measurements and the simulation are very low: with SEMCAD-X, the maximal and average deviation up to 8 cm are 1.7 dB and 0.8 dB, respectively and for FEKO the maximal and average deviations are 3.4 dB and 1.3 dB, respectively thus showing good agreement between the simulations and the measurements [10], [20].

C. Path Loss in VFM

In Fig. 2 we see that the PL is minimal at the periphery of heart because the Tx is closest to the Rx in this scenario (average distance being 12 cm) as both of them are placed on same side i.e the anterior (front side of the body) side of the body. The PL is maximal at the periphery of the right kidney as the average distance between the Tx and the Rx is 26 cm and the propagation between the antennas take place from the posterior to the anterior side of the body. Also the right kidney is heavily covered by the liver thus increasing the PL. The increase in PL depends thus on two factors: distance and the tissues and organs through which the propagation takes place. The PL in the right kidney is higher than the PL in the left kidney as the Rx is placed on the left anterior side of the body and thus the separation between the Tx and the Rx is smaller. PL in the spleen is higher than the PL in the liver due to the following reason. Although the liver and the spleen are placed almost at the same level in the human body, the liver is placed at the anterior side and the spleen is placed at the posterior (back side of the body) side. Propagation from spleen to Rx is back-to-front propagation and thus the loss increases due to the presence of various organs such as lungs and diapragm between the Rx and the Tx. While that of liver is front-to-front propagation with fewer organs present between the Tx and the Rx.

Now we will discuss the organ liver separately (similar observations are noted for other organs too).

1) Liver: The minimum, the lower quartile, the median, the upper quartile and the maximum of the PL samples obtained at the periphery of the liver all in dB are 76.62, 86.61, 91.2, 94.56, and 103.8 respectively. The positions of the Tx antenna on the periphery of the liver are as shown in the Fig. 3(a) and indicated with P_i ($i = 1 - 16$). Fig. 4 shows that the PL over the whole of liver varies depending on

the position on the periphery of the liver. In the liver at the positions $P1$, $P2$, $P3$, $P4$, PL is minimal as at these positions the link involves organs such that the attenuation is less. Also at these positions the thickness of liver is lower which is also a contributing factor for lower attenuation and less absorption of the propagation wave. PL increases for areas where the Tx antenna is fully covered by other organs. An example here is positions $P14$, $P15$, and $P16$ where the Tx is covered completely from all sides by liver, lungs and diapragm.

D. SAR in VFM

In this section the simulation results of the SAR is discussed for the various tissues surrounding the Tx antenna. ICNIRP [7] define basic restrictions to protect public from exposure to electromagnetic fields. SAR [W/kg] is defined as a measure of the rate at which energy is absorbed by the body when it is exposed to a radio frequency (RF) electromagnetic field. Compliance with the ICNIRP guidelines is investigated for the 10 g localized SAR. For a normalized input power of 1W (P_{in}) the values are shown in Fig. 6. The maximum allowed power to satisfy the ICNIRP basic restrictions (2 W/kg in 10 g of tissue) guidelines are 77, 53, 51.4, 49.3, and 64.8 mW for left kidney, right kidney, liver, spleen and heart respectively. We also list in Table IV the maximum and minumum SAR values for a power of 2 mW as it is a typical value used to carry out such a study [12]. It can be noted that the guidelines provided by ICNIRP allow a much higher use of power values. Fig. 6 shows the boxplots with the variation of the (SAR_{10g}) for each organ through its five-number description statistics, i.e, the minimum, the lower quartile, the median, the upper quartile and the maximum of the samples all in [W/kg]. The highest localized SAR occurs on the periphery of the heart and lowest on the periphery of the left kidney. SAR is highest when the organs surrounding the Tx has high conductivity. In case of the heart the Tx is surrounded by high conductive organs and tissues such as the heart ($\epsilon_r = 54.8$ and $\sigma = 2.25$ S/m) and muscle ($\epsilon_r = 50.8$ and $\sigma = 2.01$ S/m). In case of the left kidney the Tx antenna is covered at majority of times by the left kidney ($\epsilon_r = 52.7$ and $\sigma = 2.43$ S/m) and fat layer ($\epsilon_r = 5.3$ and $\sigma = 0.1$ S/m) thus having lower SAR.

1) Left Kidney: Fig. 6 shows the SAR at the periphery of the left kidney and the minimum, the lower quartile, the median, the upper quartile and the maximum of the SAR samples in [W/Kg] are 25.98, 35.29, 40, 43.66, and 46.13 respectively.. Table IV shows that the value for SAR_{10g} for a power of 3 dBm (2 mW) satisfy the ICNIRP guidelines. The maximum peak SAR_{10g} is observed around the placement of the source of the Tx antenna. The value of the SAR_{10g} depends on the dielectric properties of the organs which surround the Tx antenna. The positions on the periphery of the left kidney are as indicated in Fig. 3(b). The SAR in the left kidney for the various positions is given in the Fig. 8: the SAR decreases from position $P1$ to $P5$. This is due to the fact that at $P1$ the Tx antenna is covered both by the left kidney ($\epsilon_r = 52.74$ and $\sigma = 2.43$ S/m) and a part of the spleen ($\epsilon_r = 52.5$ and $\sigma = 2.24$ S/m) both of which are high in conductivity. As the positions of the Tx antenna, the antenna is just surrounded by the left kidney and the fat layer ($\epsilon_r = 5.3$ and $\sigma = 0.1$ S/m) and thus a reduction in SAR is observed.

E. VFM and VFB: PL model, Link budget and SAR

1) PL: Fig. 5 shows the comparison between the PL in the VFM and the VFB. PL is larger for all the organs in the VFM as compared to the VFB. The adult human is much larger than the child model thus the distance between the Tx and the Rx increases causing increase in PL. Also in case of the adult model, the organs are much more developed and larger in size as compared to the child model. PL is maximal at the periphery of the right kidney in case of both the VFM and the VFB as for both the cases the right kidney is furthest away from the Rx and it is also heavily covered under the liver. The PL is minimal at the periphery of the heart in both the human models as the heart is the closest to the Rx.

2) PL Model: The simulated results of the PL for the Tx at the various positions at the periphery of the heart, spleen, left kidney, right kidney and the liver are fitted to a normal distribution. The goodness-of-fit is validated with the Shapiro-Wilk (SW) parametric hypothesis test of composite normality with a significance lever of 5% thus showing an excellent agreement between the modeled and the simulated PL. Fig. 7 shows the cumulative distribution of the path loss for the simulations of the VFM and that of the VFB is similar. The table I lists average value (μ) and standard deviation (σ) of the modeled path loss

for the VFM and VFB. The μ values of the VFM are about 15% higher in comparison to the ones of the VFB except for the liver. In case of the liver in VFM, the Tx placed on the periphery of the liver is covered by fat layer and there exists fat layer between the Tx and the Rx. While in case of the VFB the presence of fat is very minimal in the periphery of the liver as well as between the Tx and the Rx. Due to the low conductivity of the fat layer the PL in the VFM is less than the PL in the VFB.

3) Link budget for wireless communication: We develop a link budget to check for the communication between the Tx and the Rx. The parameters selected for developing the link budget are shown in the Table II. The link budget is developed at a frequency of 2.45 GHz for an input power of 25 μW (from the European Research Council (ERC) limitation [5]). If the carrier C to noise N_0 ratio, C/N_0 of the link between the Tx and the Rx exceeds the required C/N_0 then wireless communication is possible between the Tx and the Rx.

$$Link\ C/N_0 = P_t - PL_{organ} - N_0, \tag{2}$$

$$Required\ C/N_0 = (E_b/N_0) + 10\ \log_{10}(B_r) - G_c + G_d, \tag{3}$$

where PL_{organ} is the path loss occurring in the body which also consists of the antenna losses and the antenna gain. The maximum path loss between the Tx and the Rx for each organ is specified in the Table III. To check the wireless link between the Tx and the Rx for each organ the maximum path loss is considered. In the adult VFM model the $link\ C/N_0$ exceeds the $required\ C/N_0$ (50.55 dB) for all the organs except the right kidney while in the child VFB model the $link\ C/N_0$ exceeds the $required\ C/N_0$ for all the organs. Thus in the adult model a wireless link can be established for all the organs except for the right kidney and in the child model the link can be established for all the organs. In the VFB the link is possible for all organs as the child model is smaller than the adult model and thus the distances between the Tx and Rx are smaller when compared to the VFM. In order to establish a wireless link for the right kidney in the VFM the transmit power will have to be increased. The values of the $link\ C/N_0$ and the $required\ C/N_0$ can be found in the Table III.

4) SAR: Fig. 6 shows the comparison between the maximum SAR_{VFM} (SAR in the VFM) and SAR_{VFB} (SAR in the VFB) at the periphery of the organs when the input power is 1W. $SAR_{VFB} > SAR_{VFM}$ as in the VFB the layers of fat and the muscle are thinner as compared to the VFM. In both the human models the maximum peak (SAR_{10g}) is obtained when the organs surrounding the Tx has high conductivity. In case of the heart the Tx is surrounded by high conductive organs and tissues such as the heart ($\epsilon_r = 54.81$ and $\sigma = 2.25$ S/m) and muscle ($\epsilon_r = 50.8$ and $\sigma = 2.01$ S/m). The SAR_{VFM} is minimal at the periphery of the left kidney while in the VFB it is obtained at the periphery of the right kidney. The maximum allowed power to satisfy the ICNIRP basic restrictions (2 W/kg in 10 g of tissue) guidelines are 77, 53, 51.4, 49.3, and 64.8 mW for left kidney, right kidney, liver, spleen and heart respectively for a VFM. While the maximum allowed power to satisfy the ICNIRP basic restrictions (2 W/kg in 10 g of tissue) guidelines in a VFB are 46, 64.1, 66.8, 50, and 66.2 mW for left kidney, right kidney, liver, spleen and heart respectively.

F. Placement of implant on the organ

Physicians will place the implant on the periphery of the organs without taking into account the PL obtained. However for the different positions the standard deviation (SD) and Δ, where Δ is ($PL_{max} - PL_{min}$) obtained for the organs are listed in Table V. Thus the maximum deviation that can occur when placed on any position of the organ is known beforehand. For example the deviation that is obtained when implant is placed anywhere on the liver is 6.7 dB for VFM and 8.4 dB in case of a VFB. Also from Table III it is evident that even for a power as low as 25 μW a link can be established for all organs except for the right kidney in the VFM.

We can deduce also from this study that the PL and SAR are highly dependent on the anatomy of the person and this differs from person to person. As the antennas are positioned at various locations, it is observed that the adjoining tissues play a very important role in determining the PL as well as the SAR. Adjoining tissues help in determining various effects such as increased SAR in layered tissue which cannot be observed when the SAR is assessed using homogeneous tissue simulating liquid. For example,

for larger distances between the tissue and the antenna, standing wave effects occur depending on the frequency and fat layer thickness [21]. Thus we can conclude that in order to understand better the PL and SAR variation in heterogeneous human body, an approach using antennas placed in homogeneous medium with an effective dielectric permittivity cannot provide the effects produced in layered and heterogeneous human models. However the PL in the homogeneous phantom can be used to estimate a worst case PL in the virtual family model by multiplying it with an additional factor. These PL will vary with the antennas as the PL are antenna dependent. Thus with the above research one can obtain the worst-case PL which can then be used for link budget calculations.

IV. Conclusion

A multi-implant scenario for PL and SAR is studied for heterogeneous adult and boy model for various organs such as liver, kidneys, spleen and liver. Path loss at the periphery of the vital organs depends on the distance as well as on the dielectric properties of the tissues that lies between the Tx and the Rx. The PL is maximum for organs farthest from the Rx which are the kidneys and PL is least for the heart which is closest to the Rx. The dielectric properties of the organs and tissues that lie between the Rx and the Tx also determine the PL.

Depending on the PL a link is established between the Tx and the Rx. In case of the VFM a link cannot be established from the right kidney and in case of the VFB the link can be establised between the Tx and Rx for all the considered organs. Also the standard deviation values are mentioned for the placement of the Tx on the organs when an implant is placed on any part of the organ.

The SAR_{10g} values of the organs in the VFB are higher as compared to the VFM. The SAR values depend on the dielectric property of the total organs or tissues surrounding the Tx antenna. The value of SAR increases if the organs and the tissues surrounding the Tx antenna have higher conductivity.

The PL and the SAR provided here can be used as the worst case scenario in order to carry out link budget calculations. For example if there is a implant transmitting from the liver to a receiver outside/inside

the body, one can make use of the path loss provided in this paper and use it to be a worst case scenario path loss.

REFERENCES

[1] B. S. Welch J, and Guilak F, "A wireless ecg smart sensor for broad application in life threatening event detection," in *Proc of the 26th Annual International Conference of the IEEE Engineering in Medicine and Biology Society*, 2004, pp. 3447–3449.

[2] M. Ericson, M. A. Wilson, G. L. Cote, C. Britton, W.Xu, J.S.Baba, M.Bobrek, M. Hileman, M. Moore, and S.S.Frank, "Development of an Implantable Oximetry-Based Organ Perfusion Sensor," in *Proceedings of the 26th Annual International Conference of the IEEE EMBS*, September 2004.

[3] A. Alomainy, Y. Hao, Y. Yuan, and Y. Liu, "Modelling and characterisation of radio propagation from wireless implants at different frequencies," in *Proc. of the 9th European Conf. on Wireless Tech*, Manchester, UK, September 2006, pp. 119–122.

[4] K. Sayrafian-Pour, W. B. Yang, J. Hagedron, J. Terrill, and K. Y. Yazdandoost, "A statistical path loss model for medical implant communication channels," in *Proc. of the IEEE PIMRC*, Tokyo, Japan, September 2009.

[5] V. D. Santis and M. Feliziani, "Intra-Body Channel Characterization of Medical Implant Devices," in *Proc. of EMC Europe*, York, UK, September 2011.

[6] IEEE 2005 , "IEEE standard for safety levels with respect to human exposure to radio frequency electromagnetic fields, 3 khz to 300 ghz ieee," *Std C95.1-2005*.

[7] ICNIRP, "Guidelines for limiting exposure to time-varying electric,magnetic, and electromagnetic fields," *Health Physics*, vol. 74, pp. 494–522, 1998.

[8] T. Aoyagi, K. Takizawa, T. Kobayashi, J. ichi Takada, and R. Kohno, "A statistical path loss model for medical implant communication channels," in *Personal, Indoor and Mobile Radio Communications, 2009 IEEE 20th International Symposium*, September 2009, pp. 2995–2999.

[9] A. Alomainy and Y. Hao, "Modeling and characterization of biotelemetric radio channel from ingested implants considering organ contents," *Antennas and Propagation, IEEE Transactions*, vol. 57, pp. 999–1005, April 2009.

[10] D. Kurup, W. Joseph, G. Vermeeren, and L. Martens, "Path loss model for in-body communication in homogeneous human muscle tissue," *IET Electronics Letters*, pp. 453–454, April 2009.

[11] T. Aoyagi, K. Takizawa, T. Kobayashi, J. ichi Takada, and R. Kohno, "Development of a wban channel model for capsule endoscopy," *Antennas and Propagation Society International Symposium*, pp. 1–4, 2009.

[12] M. Scarpello, D. Kurup, H. Rogier, D.Vande Ginste, F. Axisa, J. Vanfleteren, W. Joseph, L. Martens, and G. Vermeeren, "Design of an implantable slot dipole conformal flexible antenna for biomedical applications," *Accepted to IEEE Transactions on Antennas and Propagation*, 2010.

[13] M. T. H. Usui and K. Ito, "Radiation characteristics of an implanted cavity slot antenna into the human body," in *Proc. IEEE Antennas and Propag. Soc. Int. Symp*, Albuquerque, NM, p. 2006.

[14] M. T. W. Xia, K. Saito and K. Ito, "Performances of an implanted cavity slot antenna embedded in the human arm," *IEEE Trans. Antennas Propag*, vol. 57, pp. 894–899, April 2009.

[15] A. K. A Christ, T Samaras and N. Kuster, "Characterization of the electromagnetic near-field absorption in layered biological tissue in the frequency range from 30 mhz to 6000 mhz." *Physics in Medicine and Biology*, vol. 51, no. 4951, 2006.

[16] D. Kurup, W. Joseph, G. Vermeeren, and L. Martens, "In-body path loss model for homogeneous human tissues," *Accepted IEEE Transactions on Electromagnetic Compatibility*.

[17] FCC OET Bulletin 65, Revised Supplement C, "Evaluating Compliance with FCC Guidelines for Human Exposure to Radiofrequency Electromagnetic Fields," Federal Communication Commission, Office of Engineering and Technology, June 2001.

[18] R. W. P. King, G. S. Smith, M. Owens, and T. T. Wu, *Antennas in matter fundamentals, theory and applications*. Cambridge, MA : MIT Press, 1981.

[19] A.Christ, "The virtual familydevelopment of surface-based anatomical models of two adults and two children for dosimetric simulation." *Physics in Medicine and Biology*, vol. 55, no. 2, 2010.

[20] R. Verdone and A.Zanella, *Pervasive Mobile and Ambient Wireless Communications: COST Action 2100 (Signals and Communication Technology)*. Springer, 2012.

[21] A.Christ, A.Klingenbock, and N.Kuster, "Energy absorption in layered biological tissues in the near- and far-fields of the antennas of body-mounted devices," in *In proceedings General Assembly International URSI,Prog. Oral Presentations*, New Dehi, India, 2005.

Authors' affiliations

Divya Kurup, Wout Joseph, Günter Vermeeren, and Luc Martens (Ghent University / IBBT, Dept. of Information Technology, Gaston Crommenlaan 8 box 201, B-9050 Ghent, Belgium, Fax: +32 9 33 14899, E-mail: divya.kurup@intec.UGent.be)

LIST OF TABLES

LIST OF FIGURES

TABLE I

PARAMETER VALUES: NORMAL DISTRIBUTION FIT FOR THE PL IN THE VFM AND VFB AT THE PERIPHERY OF SPLEEN, HEART, LEFT KIDNEY, RIGHT KIDNEY, AND LIVER

	VFM		VFB	
Organs	μ $[dB]$	σ $[dB]$	μ $[dB]$	σ $[dB]$
$Spleen$	110.8	9.14	91.28	5.59
$Heart$	67.3	9.69	58.34	5.57
$Left\ Kidney$	130.3	6.35	114.85	6.26
$Right\ Kidney$	151.6	8.1	125.36	5.85
$Liver$	91.2	6.67	96.57	8.5

TABLE II

PARAMETER VALUES: LINK BUDGET I

Parameter	Value
Transmit power P_t [μW]	25
Transmit power P_t[dBm]	- 16
Propagation Loss Right Kidney [dB]	171.7
Propagation Loss Left Kidney [dB]	142
Propagation Loss Liver [dB]	103.8
Propagation Loss Heart [dB]	130.3
Propagation Loss Spleen [dB]	89.54
Ambient Temperature T [K]	310.0 (273 + 37)
Receiver NF [dB]	3.5
Boltzmann constant k	1.38$\times$ 10^{-23}
Noise power density N_0[dBm/Hz]	-199.70
Signal Quality	
Bit rate B_r [kb/s]	7.0
Bit error rate	1.0$\times$ 10^{-5}
Eb/N0 (ideal PSK) [dB]	9.6
Coding gain G_c	0
Fixing deterioration G_d [dB]	2.5

TABLE III

PARAMETER VALUES: LINK BUDGET II

$Required\ C/N_0\ =\ 50.55\ [dB]$		
Organ	VFM	VFB
$Heart\ Link\ C/N_0$	123.93	144.04
$Spleen\ Link\ C/N_0$	85.67	118.43
$Liver\ Link\ C/N_0$	105.74	100.93
$Left\ KidneyLink\ C/N_0$	73.95	89.42
$Right\ Kidney\ C/N_0$	44.29	76.94

TABLE IV

SAR_{10g} FOR INPUT POWER = 2MW IN VFM AND VFB

Organs	Maximum SAR [W/kg]		Minimum SAR [W/kg]		Median SAR [W/kg]	
	VFM	VFB	VFM	VFB	VFM	VFB
$Left\ Kidney$	0.092	0.09	0.052	0.087	0.08	0.093
$Right\ Kidney$	0.09	0.094	0.075	0.062	0.083	0.088
$Liver$	0.092	0.098	0.077	0.06	0.086	0.092
$Spleen$	0.094	0.095	0.081	0.079	0.087	0.09
$Heart$	0.102	0.098	0.062	0.059	0.089	0.094

TABLE V

STANDARD DEVIATION (SD) AND MAXIMUM DEVIATION (Δ) FOR THE PLACEMENT OF IMPLANT FOR EACH ORGAN IN THE VFM AND VFB

Organ	SD_{VFM} [dB]	SD_{VFB} [dB]	Δ_{VFM} [dB]	Δ_{VFB} [dB]
$Spleen$	9.1	5.6	34.6	19.63
$Heart$	9.6	5.5	38.5	26.5
$Left\ Kidney$	6.35	6.3	24.4	21
$Right\ Kidney$	8.81	5.9	34.2	21.7
$Liver$	6.67	8.4	33.4	37.4

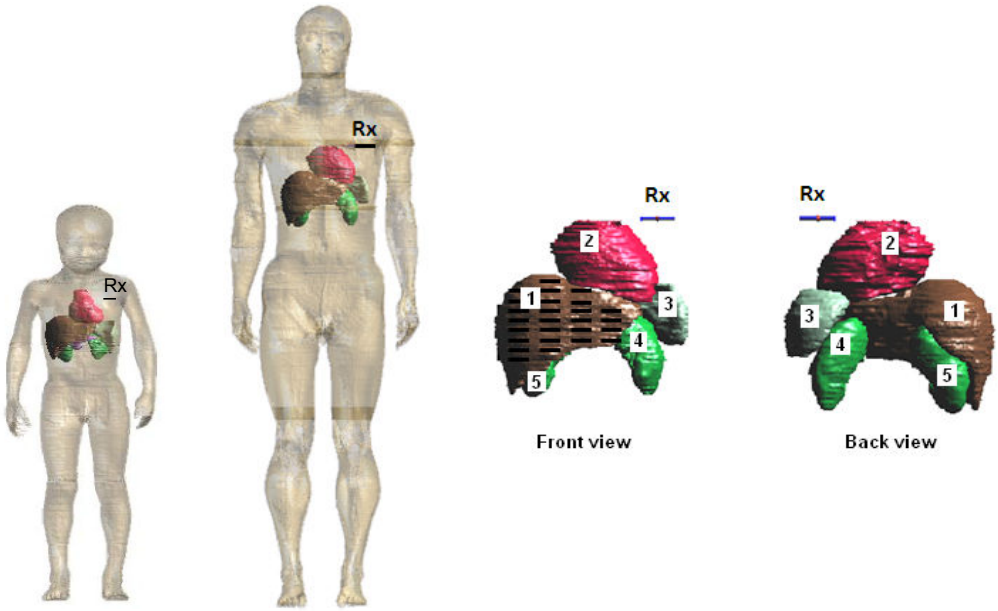

Fig. 1. Organs in VFM (1 = Liver, 2 = Heart, 3 = Spleen, 4 = Left Kidney, 5 = Right Kidney)

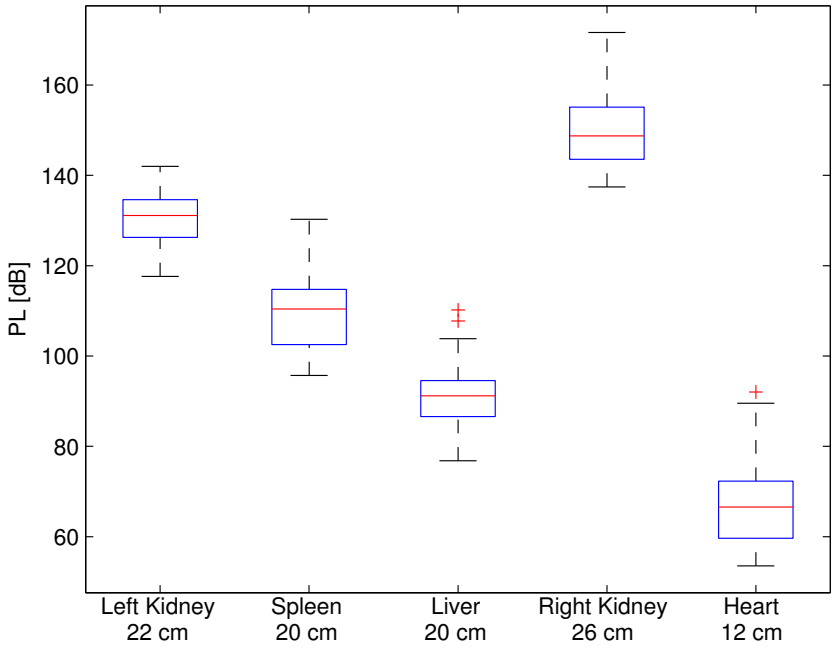

Fig. 2. Path Loss at the periphery of various organs in VFM

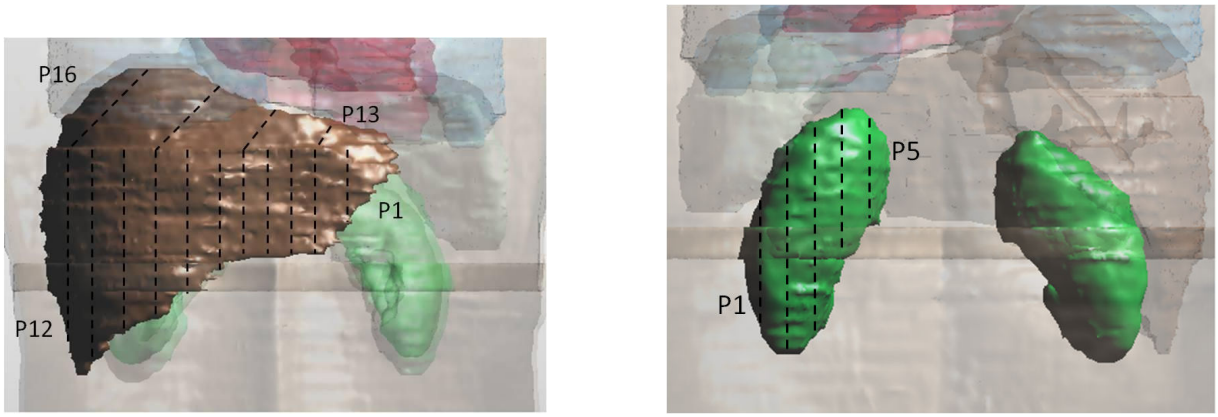

(a) (b)

Fig. 3. Positions for the Tx on the periphery of the organs in VFM: (a) Liver (b) Left Kidney

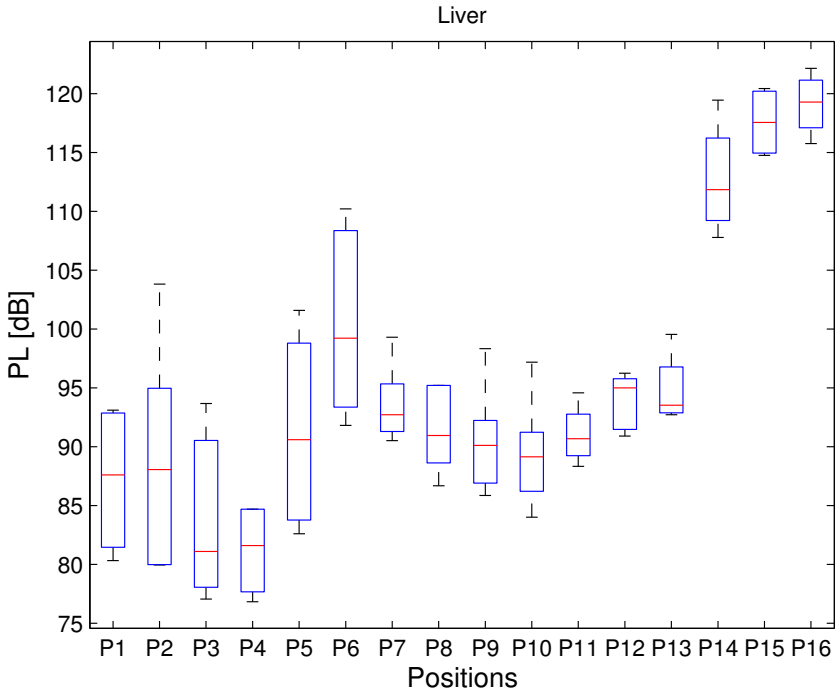

Fig. 4. Path Loss at the periphery of liver of VFM

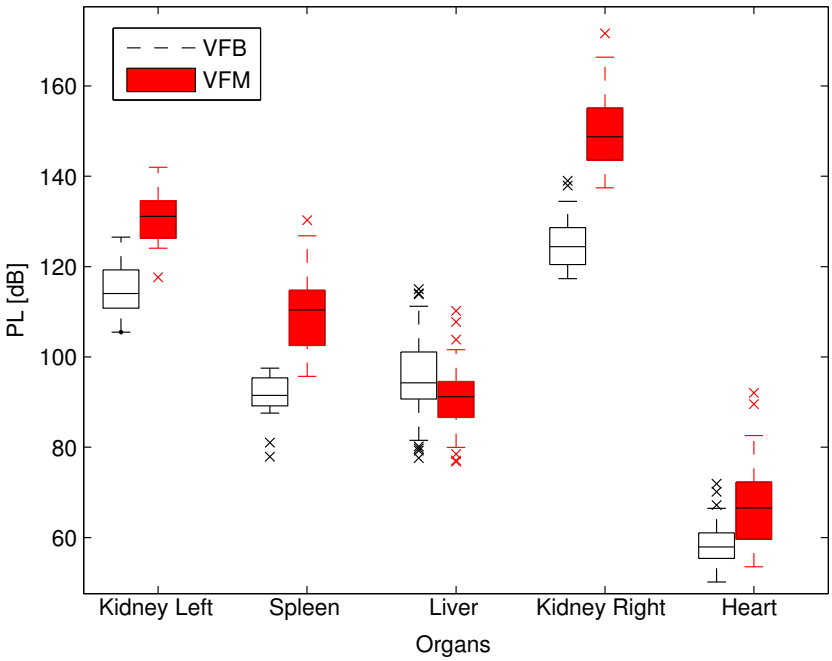

Fig. 5. Path Loss at the periphery of various organs in VFM and VFB

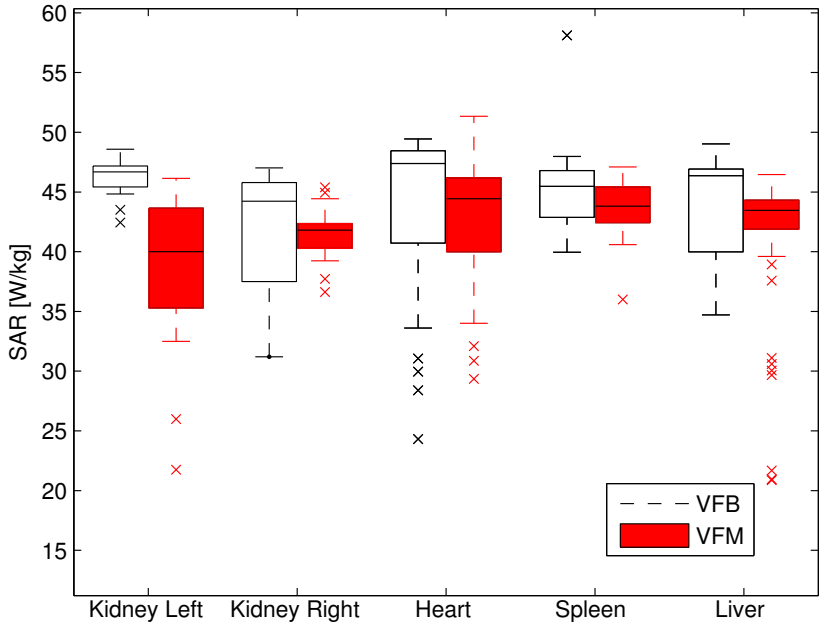

Fig. 6. SAR in the various organs in VFM and VFB (P = 1W)

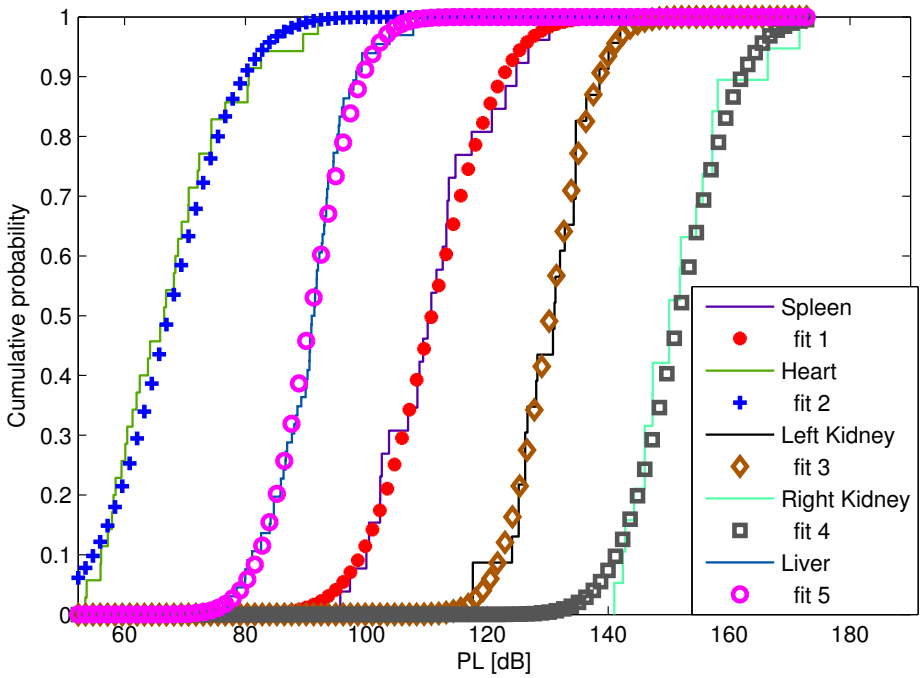

Fig. 7. Cumulative distribution of the path loss for the simulated data are fitted to a normal distribution in the VFM

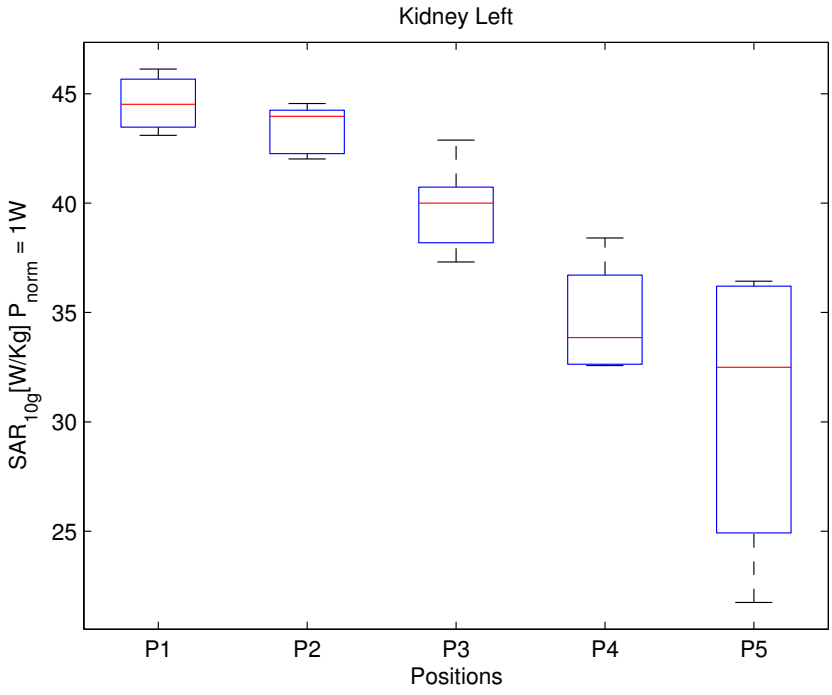

Fig. 8. SAR around the left kidney in VFM (P = 1W)